HELDA
HELSINGIN YLIOPISTO
HELSINGFORS UNIVERSITET
UNIVERSITY OF HELSINKI

UNIVERSITY OF HELSINKI

https://helda.helsinki.fi

Evaluation of Forest Features Determining GNSS Positioning Accuracy of a Novel Low-Cost, Mobile RTK System Using LiDAR and TreeNet

Abdi, Omid

Multidisciplinary Digital Publishing Institute
2022-06-15

Abdi, O.; Uusitalo, J.; Pietarinen, J.; Lajunen, A. Evaluation of Forest Features Determining GNSS Positioning Accuracy of a Novel Low-Cost, Mobile RTK System Using LiDAR and TreeNet. Remote Sens. 2022, 14, 2856.

http://hdl.handle.net/10138/349360

Downloaded from Helda, University of Helsinki institutional repository.

This is an electronic reprint of the original article.

This reprint may differ from the original in pagination and typographic detail.

Please cite the original version.

remote sensing

MDPI

Article

Evaluation of Forest Features Determining GNSS Positioning Accuracy of a Novel Low-Cost, Mobile RTK System Using LiDAR and TreeNet

Omid Abdi [1,*], Jori Uusitalo [1], Julius Pietarinen [2] and Antti Lajunen [2]

[1] Department of Forest Sciences, University of Helsinki, Latokartanonkaari 7, 00014 Helsinki, Finland; jori.uusitalo@helsinki.fi
[2] Department of Agricultural Sciences, University of Helsinki, Koetilantie 5, 00790 Helsinki, Finland; julius.pietarinen@helsinki.fi (J.P.); antti.lajunen@helsinki.fi (A.L.)
* Correspondence: omid.abdi@helsinki.fi; Tel.: +358-2941-58466

Abstract: Accurate positioning is one of the main components and challenges for precision forestry. This study was established to test the feasibility of a low-cost GNSS receiver, u-blox ZED-F9P, in movable RTK mode with features that determine its positioning accuracy following logging trails in the forest environment. The accuracy of the low-cost receiver was controlled via a geodetic-grade receiver and high-density LiDAR data. The features of nearby logging trails were extracted from the LiDAR data in three main categories: tree characteristics; ground-surface conditions; and crown-surface conditions. An object-based TreeNet approach was used to explore the influential features of the receiver's positioning accuracy. The results of the TreeNet model indicated that tree height, ground elevation, aspect, canopy-surface elevation, and tree density were the top influencing features. The partial dependence plots showed that tree height above 14 m, ground elevation above 134 m, western direction, canopy-surface elevation above 138 m, and tree density above 30% significantly increased positioning errors by the low-cost receiver over southern Finland. Overall, the low-cost receiver showed high performance in acquiring reliable and consistent positions, when integrated with LiDAR data. The system has a strong potential for navigating machinery in the pathway of precision harvesting in commercial forests.

Keywords: mobile RTK; low-cost GNSS receiver; positioning accuracy; LiDAR data; tree characteristics; terrain conditions; precision forestry; TreeNet; geographic object-based approach; commercial forests

check for updates

Citation: Abdi, O.; Uusitalo, J.; Pietarinen, J.; Lajunen, A. Evaluation of Forest Features Determining GNSS Positioning Accuracy of a Novel Low-Cost, Mobile RTK System Using LiDAR and TreeNet. *Remote Sens.* **2022**, *14*, 2856. https://doi.org/10.3390/rs14122856

Academic Editors: Yuwei Chen, Changhui Jiang, Qian Meng, Bing Xu, Wang Gao, Panlong Wu, Lianwu Guan and Zeyu Li

Received: 28 April 2022
Accepted: 10 June 2022
Published: 15 June 2022

Publisher's Note: MDPI stays neutral with regard to jurisdictional claims in published maps and institutional affiliations.

Copyright: © 2022 by the authors. Licensee MDPI, Basel, Switzerland. This article is an open access article distributed under the terms and conditions of the Creative Commons Attribution (CC BY) license (https://creativecommons.org/licenses/by/4.0/).

1. Introduction

The combination of low-cost global navigation satellite system (GNSS) with real-time kinematic (RTK) has streamlined determining centimeter-level positioning accuracy of vehicles feasible for precise practices [1,2]. However, the feasibility of this system is little known in forestry, where precision forestry is growing due to its advantages in reducing operational costs and ecological impacts.

Accurate positioning is one of the main components of precision forestry, along with remote sensing data and geospatial information systems. As forest operations become more autonomous, the demand for highly accurate positioning increases [3,4]. Machine navigation and control rely on reliable and accurate positioning to perform forest operations. On the other hand, any inaccuracy in positioning increases the costs of operations and our carbon footprint. It also decreases machine operational robustness and safety, with huge implications on the quality of production and environment [5]. Furthermore, in commercial forests, harvesters collect a huge amount of data from the processed single trees over large areas and forest stands. The data are economically valuable and include the bucking information and positions, which can be used for mapping and predicting

forest attributes [4,6]. However, any positioning errors of the data significantly degrade the performance of the models used to estimate the merchantable timber volume collected by harvesters [7,8].

Various metrics are introduced to measure the performance of GNSS positioning, such as the availability of sufficient signals, the continuity and integrity of the signals, and most importantly, the accuracy of positioning [9]. The environmental factors have an undeniable impact on the quality of signals. For example, signal blockage and multipath errors result from site-specific conditions or atmospheric factors. The poor visibility of satellites due to trees' occlusion or terrain conditions is one of the main sources of single blockage, which hampers the geometry of the GNSS and increases the optimal time for the initialization of the system [10].

Earlier studies have focused on the impact of forest type or forest cover density [11–14] in the positioning accuracy of GNSS receivers in forest environments. For example, Feng et al. (2021) [14] explored the effect of forest types and crown size on the accuracy of positioning for individual trees through GNSS receivers. They found that the error of positioning in broadleaved forests is higher than in coniferous forests, while the size of crown did show no significant impact on the increasing the error of positioning. Likewise, Murgaš et al. [13] tested the accuracy of a mapping-grade device for the positioning of inventory plots under open sky and forest canopy conditions. They reported the increase of positioning errors under canopy condition, while the coniferous forests and young stands showed lower impacts on the positioning errors of the GNSS receiver. Moreover, few studies have considered the influence of GNSS receivers' factors along with the forest-related factors. Ordóñez Galán et al. [15] tested the influence of various forest cover features and GPS-related factors on the positioning accuracy of a DGPS receiver. They reported that the influence of forest cover features on the positioning accuracy is significant in comparison with the GPS factors. However, they concluded that there is no priority between different forest variables on the accuracy of the positions. Piedallu and Gégout [16] evaluated the accuracy of GPS positioning based on the type of receiver, forest cover type, the components of GPS survey, and the season. They reported the impacts of all factors on the positioning accuracy of GPS, except the season of data recording. The influence of high density of forest cover on the accuracy of positioning is higher than other variables. However, the consideration of other factors, such as terrain variables, which may affect the positioning accuracy of GNSS receivers in a forest environment, has been somewhat diminished in earlier studies. Valbuena et al. [17] explored both terrain and forest variables. However, they excluded the terrain variables in the final modelling and concluded that the leaf area index, the relative spacing index between trees, and the wood volume can express the positioning accuracy of a GNSS receiver in a pine forest. Meanwhile, Pini et al. [1] concluded that terrain conditions are not only significant for the accuracy of positions, but are also effective for the accurate heading of vehicles. Kabir et al. [18] reported a significant decrease in in the accuracy of GNSS receivers in the mountainous areas relative to orchards or open fields. Many of these studies were developed to introduce an appropriate GNSS receiver for measuring the accurate locations of individual trees or inventory plots under forest canopy. Hence, the measurements were carried out as static, with several minutes to record an accurate position. Although positioning accuracy through mapping-grade or geodetic-grade GNSS receivers is reliable, their high cost, the difficulty in carrying them in forest conditions, and the complexity of using them have led to a degradation of their efficiency for cost-sensitive and small size applications, such as operations in precision agriculture or precision forestry. Therefore, the need for a new generation of cost-effective GNSS receivers with high positioning accuracy and simplicity of usage under forest conditions, such as u-blox modules, is inevitable.

In modern forestry, the use of high-density LiDAR data is growing for mapping the forest environment, such as individual tree characteristics [7,19,20], aboveground biomass estimation [21,22], forest disturbances [23], and logging trail detection [24,25]. Mapping forest features depends on reliable and accurate field measurements for both attributes

and positions. For this purpose, we need receivers that are able to acquire positions at centimetre-level accuracy, such as geodetic-grade GNSS receivers, to be compromised with LiDAR-derived forest metrics. However, there has also been some research that introduced the relatively expensive approaches by integrating GNSS, IMU, and mobile laser scanning (MLS) to improve the positioning accuracy for solving the simultaneous localization and mapping (SLAM) problem under forest canopy [26,27].

Despite the high positioning accuracy, the cost of establishment a traditional RTK-related receiver, e.g., a geodetic-grade receiver, is approximately 10 times higher than a low-cost RTK receiver [28], which has made it inappropriate for cost-sensitive and small size applications, e.g., in forestry or agriculture applications. The reliable accuracy and continuity of low-cost GNSS receivers are reported for a variety of applications, mostly in non-forest environments, such as surveying and mapping [29,30], monitoring [28,31], Android smartphone positioning [32], precision agriculture [2], and urban environments [33]. Many of the earlier studies reported reliable positioning of the low-cos receivers, such as u-blox modules [28–30,34–36] in a desirable environment condition, for example, an open sky with a wide range in availability of satellites. However, their efficiency might be degraded in an obstructed environment or in the dynamic mode of positioning RTK. Jackson et al. [37] evaluated the positioning accuracy of five low-cost GNSS receivers for RTK positioning under different environments, in both static and dynamic conditions. The results indicated that the positioning errors of the low-cost receivers, in static tests, was less than 10 cm in less complex areas, such as rural environments. However, the error reached over 1 m in complex areas, such as urban and suburban environments. The positioning accuracy of the receivers was different in dynamic tests, and the optimal accuracy is reported 1.5 cm to 1.8 m for the suitable receiver. Likewise, Kadeřábek et al. [2] tested the performance of various types of RTK receivers in horizontal positioning under the modes of static or dynamic. They concluded that the accuracy of positioning is significantly lower in a dynamic mode rather than a static mode. They emphasised that accelerating the speed increases the error of positioning. Janos and Kuras 2021 [35] tested the positioning accuracy of a low-cost GNSS receiver, u-blox ZED-F9P, in the RTK mode under different environment conditions. They found that the type of antenna has a significant impact on the increase of positioning errors in a complex environment, such as urban canyons.

Although a variety of studies have explored the feasibility of traditional GNSS receivers in the forest environment, our understanding concerning the efficiency of newly low-cost receivers and the factors that affect their positioning accuracy is limited, particularly in commercial forests, where the monitoring of machines or recording of the position of processed single trees by harvesters [27,38,39] has become widespread in forest operations. Hence, this research was designed to test the feasibility of using low-cost GNSS receivers and RTK correction signal to determine precise positions in forests under the rotation forest management (RFM) system in southern Finland. Specifically, we want to evaluate the positioning accuracy of the u-blox ZED-F9P in combination with high-density LiDAR data. Moreover, we will explore features that affect the accuracy of a low-cost GNSS receiver in the forest using the TreeNet algorithm.

2. Materials and Methods

2.1. Description of the Study Area

We selected three forest stands for our experiment from Karpanmaa forests in southern Finland (Figure 1). One stand is young and had undergone its first commercial thinning. Two other stands are mature and are waiting for their second/third commercial thinning operations. The tree species compositions are pine, spruce, and birch, with a predominance of pine in the three stands. The age of stands is distributed from 34 to 72 years. The height of trees is between 5 and 29 m. The ground elevation of the forest ranges between 127 and 149 m.

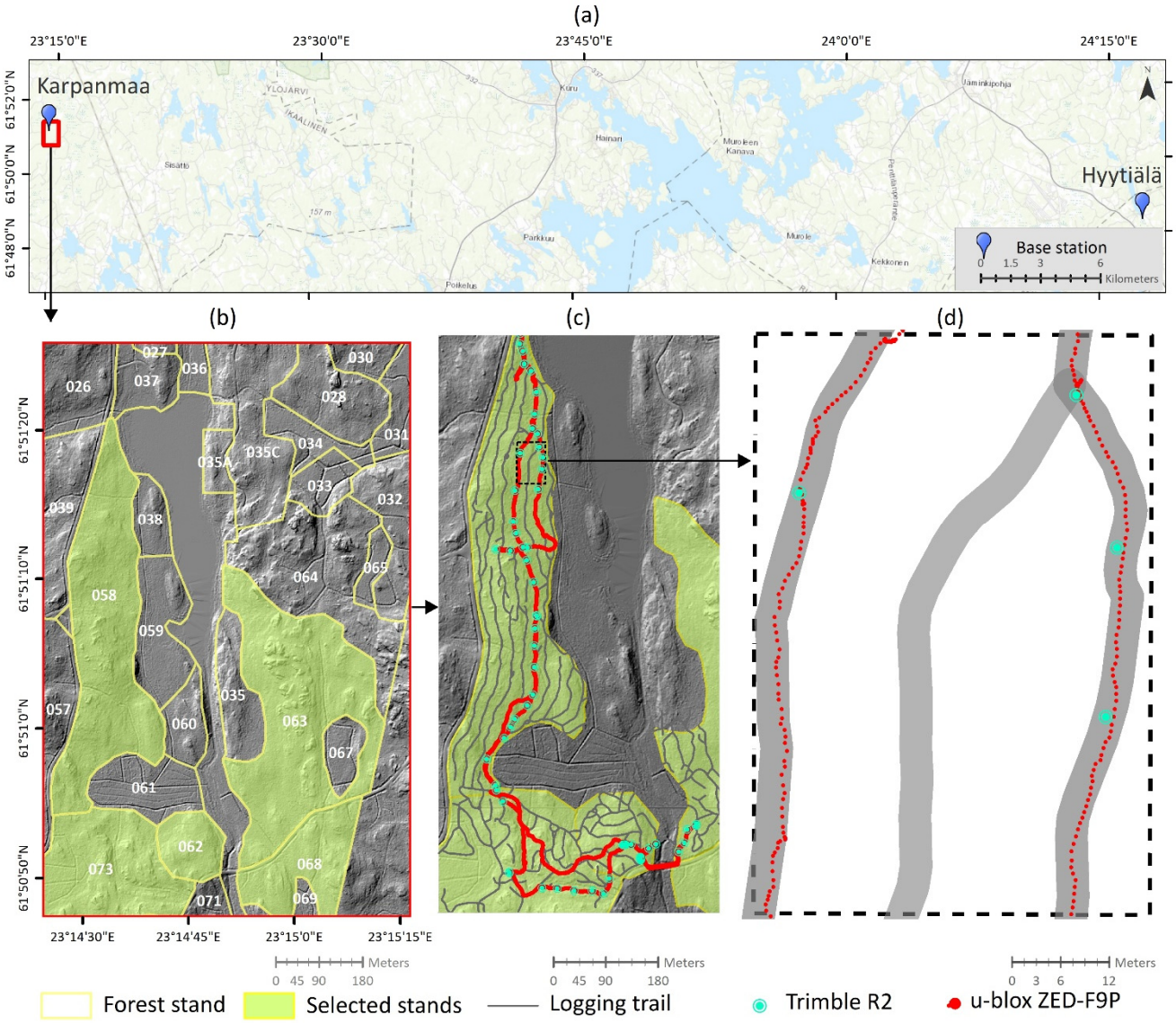

Figure 1. The study site and field measurements in southern Finland: (**a**) the locations of base stations and study area, (**b**) selected stands in Karpanmaa site, (**c**) logging trails, measured positions using the Trimble R2 and u-blox ZED-F9P and (**d**) the patterns of the recorded positions by u-blox ZED-F9P on the logging trails within an example of the study stands.

2.2. Data

We used the high-density LiDAR data, under the license of the National Land Survey of Finland (NLS), recorded in 2020 for the selected stands. The data have a density of greater than 5 points/m^2 along with horizontal and altimetric errors of less than 45 and 10 cm [40], respectively. The features affecting the positioning accuracy of the u-blox ZED-F9P were mapped from the LiDAR-derived metrics such as the digital terrain model (DTM), digital surface model (DSM), point density, and signal intensity. Logging trails were detected from the high-density LiDAR data based on the U-Net convolutional neural network approach developed by Abdi et al. [25]. In addition, we obtained orthophotos from the databases of NLS [41]. The attributes of the forest stands were collected from the databases of Finsilva Oy.

2.3. GNSS Devices

Three GNSS receivers were used, including an Oregon® 750t (Garmin Ltd., Olathe, KS, USA), a u-blox ZED-F9P (u-blox, Thalwil, Switzerland), and a Trimble R2 (Trimble Inc., Sunnyvale, CA, USA), for specialised applications during our field operations.

The Oregon® 750t receiver was used for navigating the approximate locations of the selected logging trails.

We used the u-blox ZED-F9P to identify features affecting the positioning accuracy of the low-cost GNSS receivers in the forest. The u-blox ZED-F9P is a multi-band GNSS receiver that can measure positions at centimetre-level accuracies in RTK mode. This receiver obtains signals from multiple bands (L1, L2/E5b/B21) of all four global GNSS constellations including GPS, Galileo, BeiDou, and GLONASS via a Multi band GNSS antenna ANN-MB-00 (SMA) (u-blox, Thalwil, Switzerland) [42]. The antenna is designed in a small, compact size. It can be easily mounted on different machinery due to its magnetic fixed installation base and a long cable of 5 m [43]. The GNSS and RTK integration has accelerated its convergence time (down to less than 10 sec) [42]. Moreover, performance with the application for conducting unmanned autonomous vehicles (UAV), automatic and semi-automatic machinery, and robotic machines has improved [44]. The u-blox F9P was equipped with advanced anti-spoofing and anti-jamming algorithms that guarantee highly accurate positioning and navigation information. The receiver and antenna are both waterproof and can also operate under extreme temperatures (−40 °C to +85 °C) [45].

We used the Trimble R2 receiver, paired with Trimble TSC7 (Trimble Inc., Sunnyvale, CA, USA), for collecting accurate control points during recording data through u-blox F9P. The Trimble R2 can acquire high positioning accuracy in RTK mode both horizontally (1 cm to 1 ppm RMS) and vertically (2 cm to 1 ppm RMS).

2.4. Research Sulky

We modified a sulky for transporting the u-blox and its compartment for recording positioning data in the forest. The sulky includes two bicycle wheels of 28″ in width. The length, width, and height of the main body of the sulky are 1.2 m, 65 cm, and 87 cm, respectively. It was equipped with a veneer plate (103 cm × 53 cm) for holding the devices. A thin plate (50 cm × 40 cm) was installed on the veneer plate for fixing the magnetic antenna. The sulky was controlled by a draught pole (adjustable up to 1.3 m), which includes a trapezoid-shaped handle to make pulling easier for the user (Figure 2).

2.5. Field Measurements

We established the local base stations to send corrected data to the rover receiver in the vicinity of our study site (Figure 1a). The base and movable stations were developed using a SparkFun GPS-RTK2 Board (SparkFun Electronics, Boulder, CO, USA) with ublox-ZED-F9P module and the SMA. The receivers of the base stations were configured based on an NTRIP-protocol via the internet server (rtk2go.com) to provide RTCM V3.2 standard correction signals.

We selected a number of logging trails with about 2 km for our experiment (Figure 1c). The shapefiles of the logging trails were converted into GPS Exchange Format (GPX) and imported into the Garmin device for spotting out the logging trails in the field.

We started our measurement from 8:32 a.m. and ended at 12:37 p.m. (GMT). The routes were so designed to pass through different species with diversity in age, height, density, canopy cover, and topographic conditions. Our speed was close to the normal speed of harvesters and forwarders (i.e., 44 to 56 m/min) in the forest.

The u-blox ZED-F9P receiver and its compartments, including the SAM, 4G TP-LINK M7200 modem (TP-Link Technologies Co., Shenzhen, China), and Laptop computer, were mounted on a research sulky that was designed for this purpose (Figure 2). The configuration period of the receiver was set to 1 Hz. All four GNSS constellations were selected to receive adequate and strong signals to acquire positions by the u-blox F9P in RTK mode. A Raspberry Pi minicomputer with RTK-LIB open-source program was used for

operating the RTK-station. We used u-center evaluation software program to monitor and process all aspects of recorded data (e.g., horizontal and vertical positions, accuracies, time, tracking of GNSS constellations, etc.) during the operation of the u-blox GNSS receiver [46]. All recorded data were captured in ASCII format, imported into ArcGIS (Esri, Redlands, CA, USA), and integrated with the object features to be used for TreeNet analysis.

Figure 2. Compartments for field experiment: (**a**) research sulky, (**b**) u-blox ZED-F9P, (**c**) Multi band GNSS antenna ANN-MB-00 (SMA), (**d**) modem, and (**e**) computer system.

We recorded the positions of 64 control points on the logging trails with an accuracy of less than 1 cm by the Trimble R2, as references, in RTK mode. The absolute errors were calculated between the measured positions by the u-blox F9P and the positions of the control points. The one-sample t-test was used to determine whether the mean of errors exceeded the optimal directions of an image pixel (i.e., 50 cm) derived from the high-density LiDAR data at a significance level of 0.05.

2.6. High-Density Laser Scanning Features

We applied the binning interpolation method based on the maximum cell-assignment method to generate a digital surface model (DSM) from the high-density LiDAR points. The linear interpolation method was used to fill void areas in the DSM. The digital terrain model (DTM) was created based on the interpolation from ground points as well [47]. The features representing the surface topography and canopy conditions, such as slope gradient, aspect, topography/canopy position, plan curvature, profile curvature, and mean curvature [48,49], were derived from the DTM and DSM (Figure 3).

We subtracted the DTM from the DSM to reach the canopy height model (CHM) [50]. The canopy density was generated based on the ratio of the number of nonground points to the total number of points in an object [51]. The tree canopy was delineated from the CHM and used for measuring the canopy cover within an object [52]. The intensity image was created from the range of pulse-intensity values of the laser points [53]. It was applied in combination with orthophotos to determine species types within the objects.

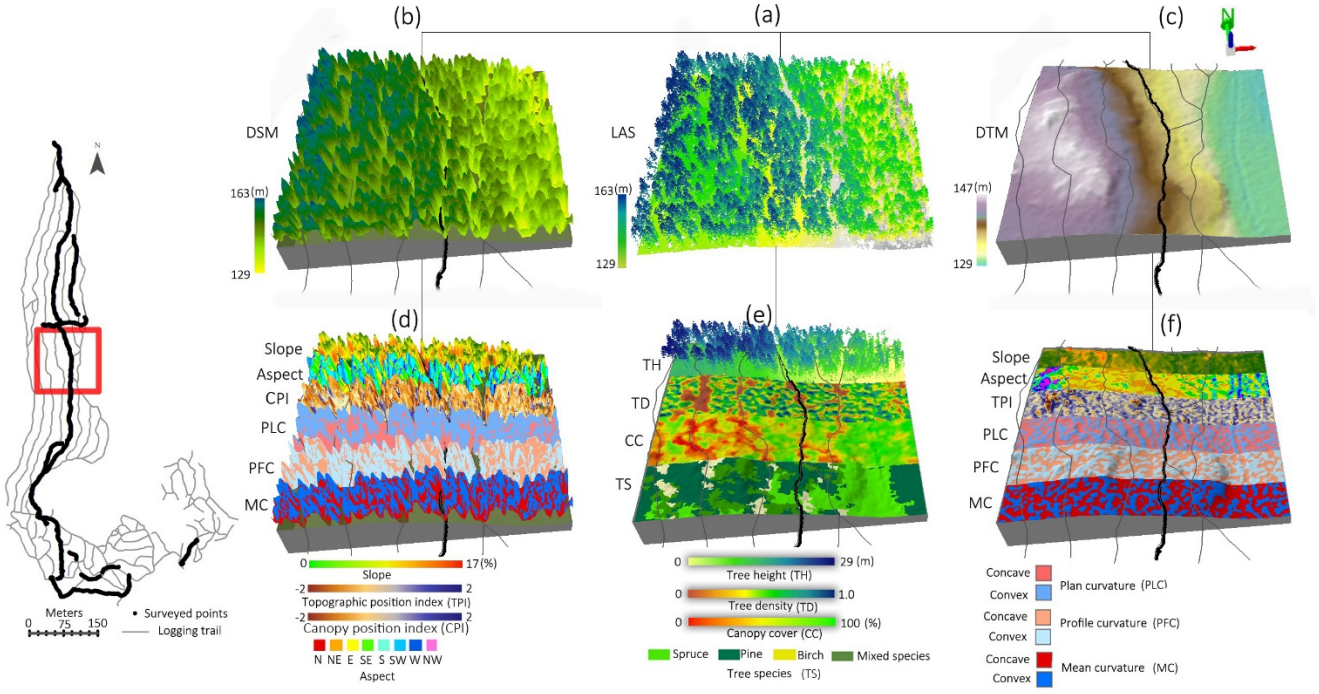

Figure 3. Object features in an example area of the study area. (**a**) 3D perspectives of high-density LiDAR point clouds, its metric derivatives including (**b**) the digital terrain model (DTM) and (**c**) digital surface model (DSM). (**d**) The ground-surface features were extracted from the DTM and (**e**) the canopy characteristics and (**f**) the canopy-surface features were extracted from the LiDAR points and the DSM, respectively.

2.7. Object Features

A buffer of 10 m was delineated around the logging trails, and then the area was segmented into the homogenous units (objects) based on the similarity in the spectral properties of the adjacent cells in the high-resolution orthophotos. The average size of the objects was obtained around 18 sq.m. The values of the derived features from the LiDAR data (Table 1) and the accuracy of positioning by u-blox ZED-F9P were summarized within the objects. This single database was used for analyzing the relationship between the target and the features using TreeNet.

2.8. TreeNet Regression

We used the TreeNet regression algorithm to determine influential features on the positioning accuracy of the u-blox ZED-F9P. Numerous advantages have been reported for TreeNet, in comparison with other machine learning based approaches. In addition to its highly accurate predictions, TreeNet is not sensitive to errors in data or missing data. No data pre-processing (e.g., transformation, normalisation, or reduction) or preselection of the variables is required. TreeNet is strong against overfitting, and the process of growing trees is extraordinarily fast [54,55].

TreeNet begins with an initial model, which consists of a very small tree. This simple model is deliberately weak. The residuals are computed for each data in the first model and are used to grow the second tree. The residuals of the second tree are then computed and used to grow the third tree. Likewise, this process repeats to generate a sequence of hundreds or thousands of trees, in order to achieve an optimal tree. All trees contribute to the optimal model. The final model prediction is based on the total contribution of the individual trees, which is known as score. The accuracy of the TreeNet score will improve steadily by increasing the number of trees until to reach an optimal number of trees [55].

We used a dataset including 2000 sample objects. Twenty percent of the sample objects were randomly assigned as the testing set and the remaining 80% as the learning set. The

TreeNet loss function was set on Huber-M. The mean square error (MSE) was chosen as the criterion for determining the number of optimal trees. We set the initial tree size at 10,000 and generated 12 TreeNet models based on the different learning rates and tree complexity levels. The optimal model was selected based on the one that recorded the minimum MSE, and its parameters were tuned for the final TreeNet model. The performance of the model was tested using the area under the receiver operating characteristic (ROC) curve. A value greater than 0.9 represents high performance, while values less than 0.7 indicate low performance [56] of the TreeNet model.

The influence of features on the positioning accuracy of the u-blox ZED-F9P was determined via relative importance [55]. The importance values of the features are ranged between 0 and 100. The most influential feature gains a value of 100 and the remaining features are rescaled to reflect their importance relative to this feature. We produced partial dependence (PD) plots for individual and pairs of features that contributed to the predicted positioning accuracy in the model. The PD plots represent the response of the target variable to individual or pairs of features, as all remaining features are taken into account [57].

Table 1. Object features affecting on the accuracy of positioning by u-blox ZED-F9P, derived from different metrics of high-density LiDAR data.

Category	Features	Description
Ground-surface/canopy-surface conditions	Elevation	The mean of ground/canopy elevation (m) [58] in an object.
	Slope (°)	The average of maximum changes in elevation value [59] within each object.
	Aspect	The direction of compass of downhill slope [59] in each object.
	Topographic position index (TPI)	TPI measures the difference between the elevation of the central point against the average elevation of the ground surface in an object. The positive values indicate the higher elevation of the central points and vice versa [60].
	Canopy position index (CPI)	CPI measures the difference between the elevation of the central point against the average elevation of the canopy surface in an object. The positive values indicate the higher elevation of the central points and vice versa.
	Plan curvature	The curvature of the surface (ground or canopy) perpendicular to the direction of slope. The positive values indicate the convex surface and negative values indicate the concave surface [48,49].
	Profile curvature	The curvature of the surface (ground or canopy) in the direction of the maximum slope in each object. The negative values indicate the convex position and positive values indicate concave surface [48,49].
	Mean curvature	The combination of the plan and profile curvatures within an object [48,49].
Tree characteristics	Canopy height	The difference between the elevation of canopy surface and ground surface in an object [50].
	Canopy density	The density of nonground returns of LiDAR points in an object [51].
	Canopy cover	The percentage of canopy cover within an object, delineated from the CHM [52].
	Species type	The type of species trees extracted from the intensity image, derived from the high-density LiDAR data and orthophoto images.

3. Results

3.1. The Accuracy of Positions

The mean of absolute errors of positions between those measured by u-blox ZED-F9P and control points was obtained as about 43 cm. The result of the one-sample t-test showed that the positioning accuracy of u-blox has no significant deviation from the area of logging trails (test value = 0.5 m, p-value > 0.05). However, the absolute errors are distributed between 1.5 cm to 1.8 m (Figure 4).

Figure 4. Distribution of absolute errors of positions recorded for u-blox ZED-F9P in control points.

3.2. TreeNet Performance

The optimal TreeNet model was obtained after building 490 trees with a learning rate of 0.011 and tree complexity of 7 (Figure 5). The ROC values were 0.977 for the training dataset and 0.745 for the testing dataset. It indicates that TreeNet demonstrated high performance for expressing the features that are determining the positioning accuracy of the GNSS receivers in forest.

3.3. Features' Importance

The results of evaluation the importance values of features indicated that all of the features have affected the positioning accuracy of u-blox ZED-F9P. The top influential feature was tree height. Then, the influential features were ranked by their importance to the tree height feature. The ground elevation and aspect have gained 79% and 62% importance of the tree height, respectively. The importance of the other features has steadily decreased from the canopy surface elevation to the surface aspect. Two out of five top influential features were classified in the category of tree characteristics (Figure 6).

3.4. Marginal Effect of Individual Features

The interpretation of univariate PD plots regarding the tree characteristics shows that when tree height increases to 14 m, the error in positioning by u-blox ZED-F9P increases (Figure 7a). By increasing tree density, the positioning error drastically increases, at a density over 0.25 (Figure 7b). Canopy cover of more than 30% shows a positive response to error in positions of the GNSS receiver (Figure 7c). The mixed species and pine show a positive response to the high number of errors among tree species (Figure 7d).

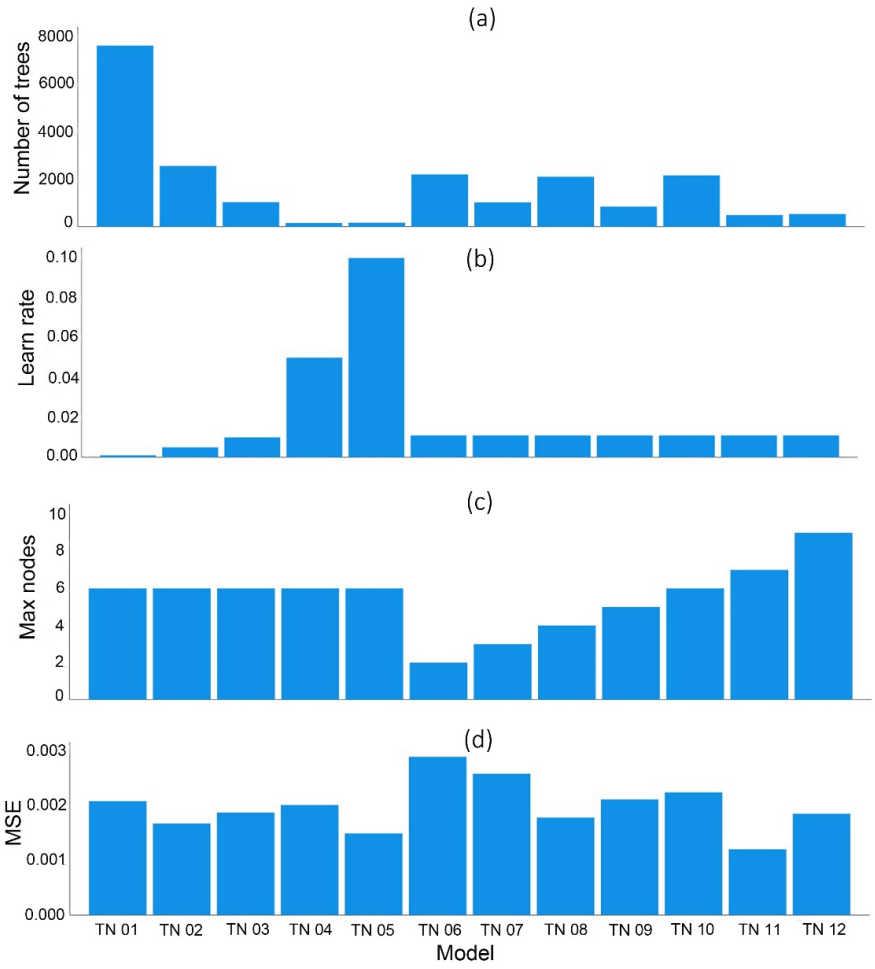

Figure 5. Comparison between different TreeNet (TN) models regarding (**a**) the number of trees, (**b**) learning rates, and (**c**) tree complexity for determining optimal TreeNet model based on (**d**) the mean square error (MSE).

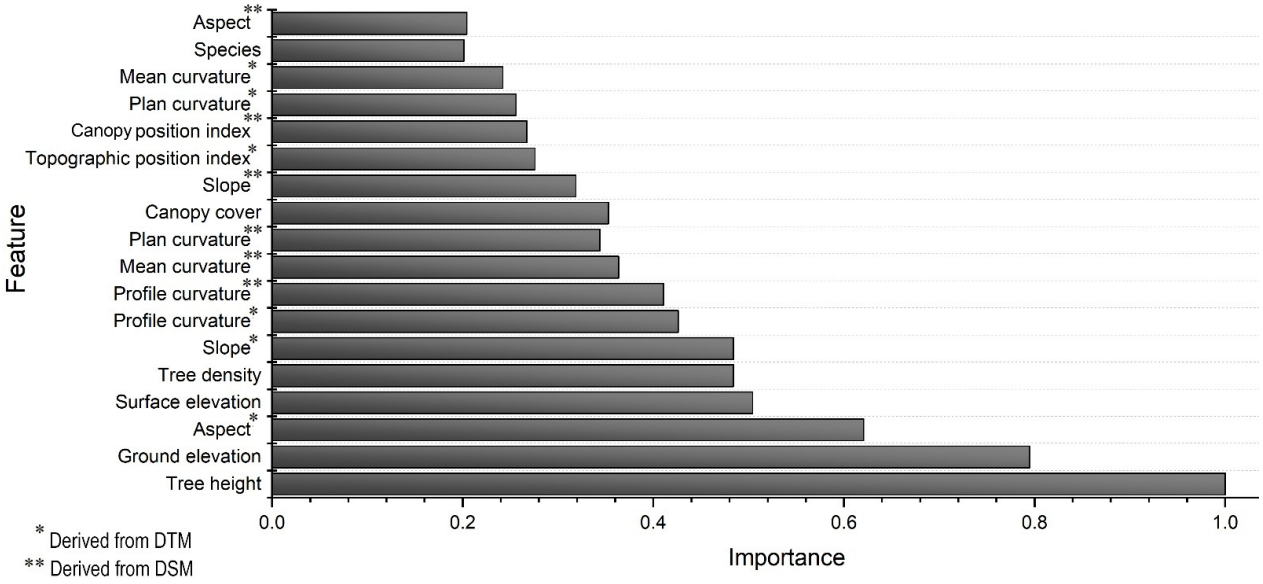

Figure 6. Importance scores of the features affecting the positioning accuracy of u-blox ZED-F9P. The top influential feature is tree height. Other features are ranked based on their importance to the tree height.

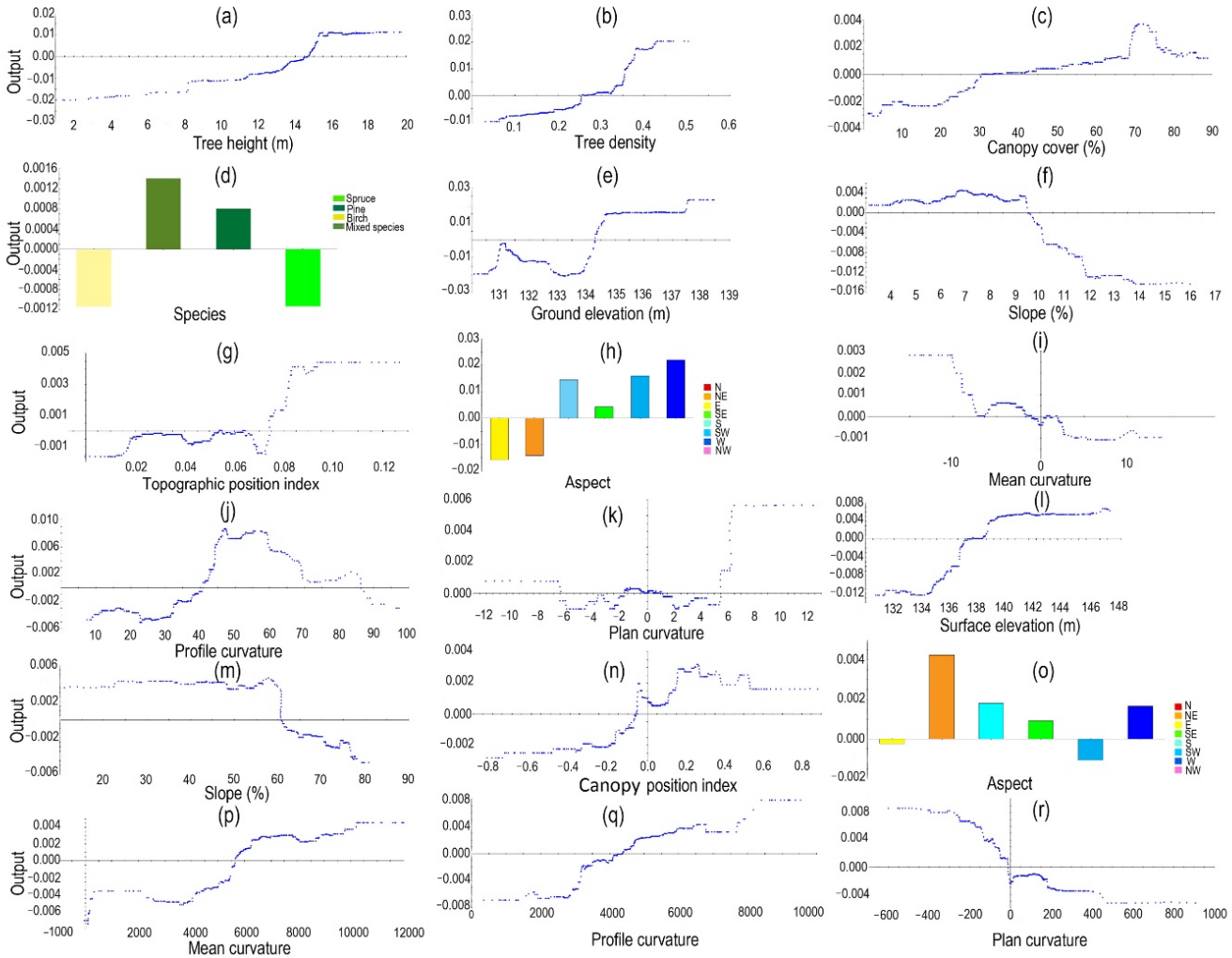

Figure 7. Univariate partial dependence plots for features affecting the positioning accuracy of the u-blox ZED-F9P. (**a**–**d**) tree characteristics, (**e**–**k**) topography conditions, and (**l**–**r**) canopy-surface conditions.

The univariate PD plots of the topographic features show that, when the ground elevation exceeds 134 m in the study area, the error of positioning by u-blox increases (Figure 7e). The areas with a slope of less than 10% show a positive response to the errors (Figure 7f). Increasing complexity in the topographic position increases the errors (Figure 7g). The western direction shows the greatest errors among the topographic aspects. The southern, south-western, and south-eastern directions show a positive response to the errors (Figure 7h). The concave curvatures show a positive response to errors in plan, profile, and mean curvatures (Figure 7i–k).

The PD plots show that the surface elevation positively responds to the high error in recorded positions by u-blox ZED-F9P after 137 m (Figure 7l). The areas with a surface slope of less than 60% show an increase in the errors (Figure 7m). High complexity in the canopy-surface position coincides with high errors in positioning (Figure 7n). Canopies with the domination of the north-eastern direction show higher errors (Figure 7o). The canopies with concave curvatures demonstrate mostly high errors totally, vertically, and horizontally (Figure 7p–r).

3.5. Marginal Effects of Pairs of Features

Figure 8 shows the interactions of five top pairs of features on the positioning accuracy of u-blox ZED-F9P. The increasing height of trees (Figure 8a), tree density (Figure 8c), surface elevation (Figure 8f), and ground elevation (Figure 8j) in the western and southern

portions increased the probability of errors in the receiver. The interaction of large trees and high tree-density (Figure 8b), surface elevation (Figure 8d), and ground elevation (Figure 8g) increased the errors. The interaction of increasing the tree density and surface elevation (Figure 8e) and ground elevation (Figure 8i) led to errors in positions. Whenever both ground elevation and surface elevation increased, the errors increased (Figure 8h).

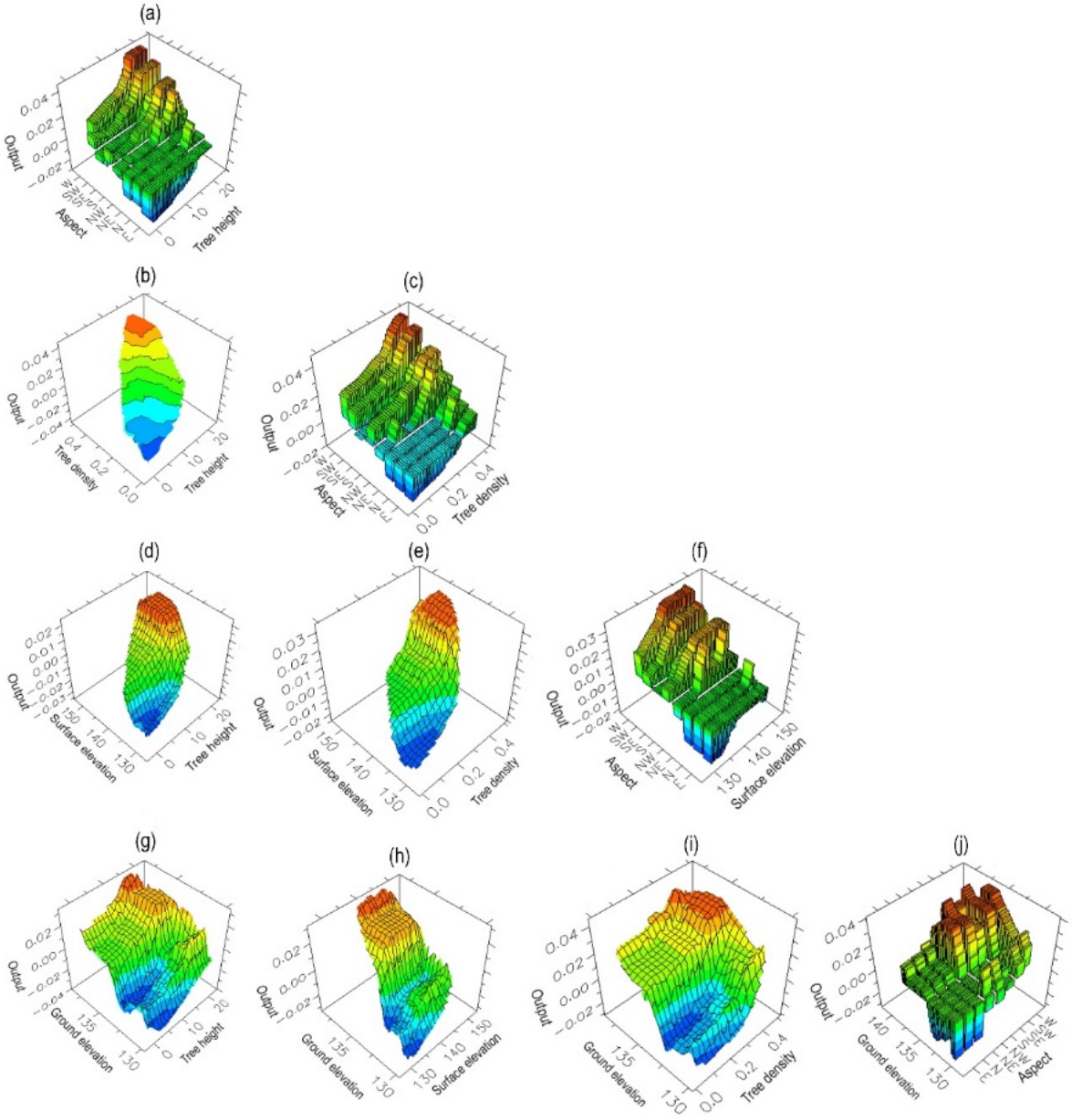

Figure 8. Bivariate partial dependence plots for five top features affecting the positioning accuracy of the u-blox ZED-F9P. (**a**) tree height and aspect, (**b**) tree height and tree density, (**c**) tree density and aspect, (**d**) tree height and surface elevation, (**e**) tree density and surface elevation, (**f**) surface elevation and aspect, (**g**) tree height and ground elevation, (**h**) surface elevation and ground elevation, (**i**) tree density and ground elevation, and (**j**) aspect and ground elevation.

4. Discussion

4.1. The Positioning Accuracy of the Low-Cost GNSS Receiver

We reach an absolute error of 0.43 m for positioning accuracy by the low-cost u-blox ZED-F9P GNSS receiver with its equipped standard patch antenna in movable RTK mode in forest environment. This level of positioning accuracy is promising for forest operations, particularly relative to the positioning accuracy of current GNSS receivers used by vehicles

in forest. Alternatively, the development of LiDAR systems has provided the possibility of producing high precision maps of the forest environment and tree characteristics at centimetre-level accuracy, with a significant reduction in costs and improvement in time of processing. Our findings verify the trust in positioning by the low-cost receiver in RTK mode for integration with the forest features derived from high-density LiDAR data, such as logging trails. This may have wide implications for the improvement of the safety of crews, autonomous navigation, ergonomics, and reduction of environmental impacts and costs [61] during forest operations down the pathways of precision forestry. Although the positioning accuracy of the low-cost GNSS receivers in static mode was reported higher than the RTK mode in complex non-forest environments [2,37], their positioning accuracy was considerable in this mode [28,30] as well. We should stress that our results are only based on using the standard patch antenna. Further work is required to test the performance of the low-cost GNSS receivers when equipped with additional antennas in the forest environment. Previous experiments acknowledged significant improvement in the positioning accuracy of the low-cost receivers, for example, when using with a geodetic-grade antenna [29,34,35].

The u-blox ZED-F9P obtains signals in multiband from four global GNSS. Multi-GNSS contributes to increasing the continuity and integrity of positioning by the receivers, particularly in environments with obstacles [62,63]. The effect of receiver types on the accuracy of positioning was reported in earlier studies. The survey-grade devices recorded higher accuracy than consumer-grade [16,64], mapping-grade [13,65], or smartphone-grade [66–68] devices.

4.2. The Performance of TreeNet

This study applied high-density LiDAR data and a novel object-based TreeNet approach to determine influential features that degrade the positioning accuracy of the novel developed low-cost GNSS receivers in a forest context. Earlier studies mostly modelled the influential variables of positioning accuracy using traditional regression models [12,14,17,66], which are limited with few variables and data. Conversely, we adopted TreeNet, as one of the most powerful machine learning algorithms, with remarkable abilities in handling big data and numerous variables without any preselection, pre-processing, or reduction in dataset. It reveals that a combination of forest characteristics and terrain features express the positioning errors of GNSS receivers. However, the importance of features are different.

4.3. Influential Forest Features

Based on our analyses, LiDAR-derived tree height is the top feature that influence on the positioning accuracy of the low-cost GNSS receiver in movable RTK mode. Tree density is among top five influential features (Figure 6). The complexity of the forest structure causes multipath effects [69], which is one of the main sources of increasing positioning errors in forest. Tree's characteristics, such as height, volume, tree density and canopy may block or weaken the signals [70]. A closed canopy can cause cycle slips [63], which clogs the signals to reach the receivers. Our analyses demonstrated that the low-cost GNSS receiver continuously recorded the signals throughout the logging trails, and it was resistant against cycle slips effects. Conversely, the great majority of work has focused on the canopy cover [11,13,14,16,71–73] as the main factors that affect the positioning accuracy of the GNSS receivers. Nevertheless, no priority between the forest cover factors on the positioning accuracy of GNSS was reported in the research of Ordóñez Galán et al. [15], while our study shows that there is a distinct difference between the impacts of tree characteristic factors on the positioning accuracy of the GNSS receiver. Moreover, some earlier studies reported the higher impact of the broadleaved tree species on increasing the errors of positioning by the GNSS receiver [13,14]. Our research showed that the importance of the tree species is less than other tree characteristics. The influence of pine and mixture species is positive against the spruce and birch.

Using high-density LiDAR data enabled us to take into account precisely some features of tree characteristics that were less a focus of earlier studies, such as tree height or tree density, not in plot scale but over the entire surveyed logging trails. For example, due to limitations involved in using traditional methods to measure tree height, the preponderance of the studies focused instead on forest cover or forest type [13–16,64] as potential effective factors of tree characteristics to determine the positioning accuracy of GNSS receivers. We considered trees' characteristics inside an object, which is much more similar to the natural condition of a forest stand. Furthermore, we carried out the experiments in a season which the leaf of some tree species such as birch is almost off. Hence, canopy cover or tree species did show lower importance than tree height or tree density in the current research. Likewise, topographic conditions affect the signals and cause the multipath effects. Our study revealed that topography directions and elevation are among top five important features that determine the positioning accuracy of the low-cost GNSS receiver (Figure 6). Aspect and slope derived from the DTM showed higher importance than was shown by the corresponding features derived from the DSM. The high ability of DTM to visualise the morphology of the bare earth under the forest canopy [74], such as variations in slope directions and values, might be one reason for this difference. On the other hand, the high variation in the curvature of the forest canopy may lead to a higher influence of DSM-derived plan curvature and mean curvature when compared to the corresponding derivatives from the DTM. Although there is no holistic research about the impact of topographic conditions in forest environment, some studies verified significant impacts of terrain in non-forest environments on the positioning accuracy of the GNSS receivers [1,18]. Based on the PD plots, the positioning errors of the low-cost GNSS receiver increase in forest areas with tree height above 14 m, tree density above 30%, western topographic directions or high elevation (Figure 6). These thresholds are based on our results in southern Finland, and similar studies should be repeated to achieve fixed values over the Nordic region. The performance of the antenna, as a sky view, is presented for a specific measured position during our experiment in Figure 9. The number of satellites that are used in navigation with a valid fixed position in the eastern direction is higher than in the western direction. We can infer that the geometric location of the satellites and their signal qualities may cause that aspect to be one of the top features determining the accuracy of the positioning by the low-cost GNSS receiver. Lower fixing rates and position errors of GNSS on west aspects were reported by D'eon and Delparte [75]. However, they reported that the differences in these values between different directions were not significant. The effect of aspect and convex slopes on the odds of missing signals was reported in the forest as well. Zimmerman and Keefe [76] verified that the alert delay of GNSS in the west directions is higher than in the east directions, which increases the error of positioning under forest canopies.

In addition, our analyses indicated that the interaction of the conditioning features intensifies the positioning errors by the receiver (Figure 8). It seems that using extra antenna or geodetic antenna [29–31,35] may mitigate the impact of the forest structure or topographic conditions on the positioning errors of this type of low-cost GNSS receivers in forest environments.

4.4. The Application

The new generation of harvesters is equipped with sensors, computers, and GNSS receivers that store big data obtained from the processed trees and machine parameters as a standard format of StanForD (Standard for Forest Data and communication) [3]. Despite the high capacity of these data for modelling forest productivity, the errors in positions significantly degrade the efficiency of these data [6–8]. This type of low-cost GNSS receiver can improve the accuracy, integrity, and continuity of positions for the harvesters, with a significant impact on increasing the efficiency of forest productivity maps to Improve the sustainability of future rotations and precision forestry. Moreover, understanding the influential features that affect the positioning accuracy of the low-cost GNSS devices contributes to developing algorithms for the correction of positioning errors

or for the selection of appropriate low-cost receivers or antennas to minimize the influence of environmental features on positioning accuracy during forest operations.

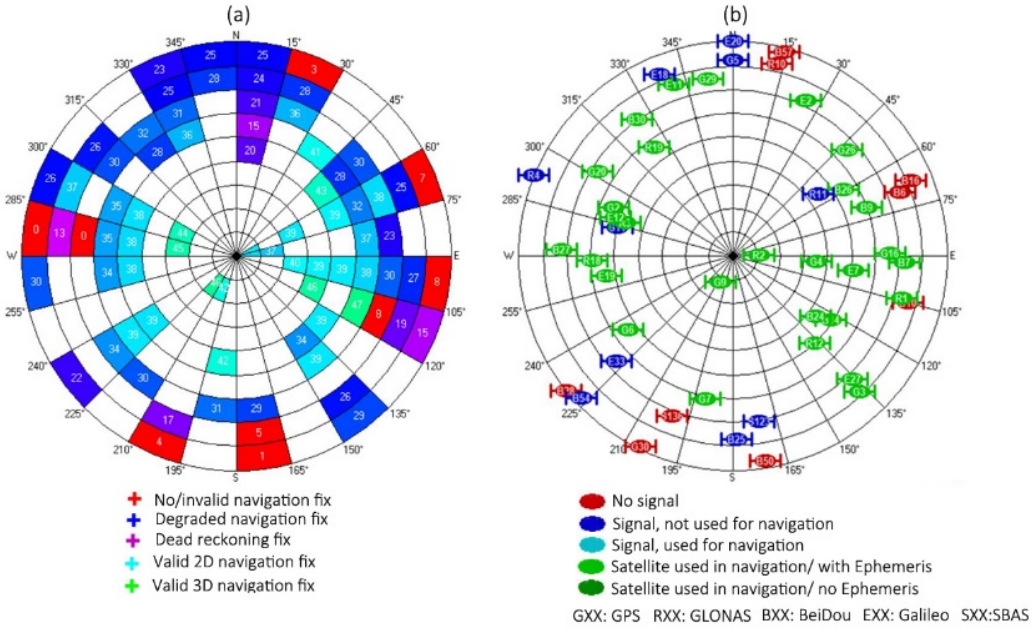

Figure 9. Sky view for a specific location for the antenna of u-blox ZED-F9P: (**a**) the quality of sky view and (**b**) the position of satellites that were used in navigation.

5. Conclusions

In this study, we presented a geographic object-based TreeNet approach to determine influential environmental features that affect the positioning accuracy of a newly developed, low-cost, high-precision GNSS receiver, u-blox ZED-F9P, in forests. The experiment concentrated on some logging trails in commercial forests in Southern Finland. The low-cost receiver showed reliable positioning accuracy when integrated with high-density LiDAR data in the forest. The TreeNet model showed a high performance for expressing features that determine the positioning accuracy of the low-cost receiver in the forest. A combination of features increased the positioning errors of the low-cost receiver, in which the most important feature was tree height and then the topographic features, such as elevation and slope direction over the study stands. In the current research, we merely used the standard patched antenna packed with the low-cost receiver. However, we suggest testing the efficiency of other types of antennas, e.g., geodetic-grade ones, or a combination of antennas with the low-cost receiver to improve the positioning accuracy in the forest environment.

Author Contributions: Conceptualization, O.A., J.U., A.L. and J.P.; methodology, O.A., J.U., A.L. and J.P.; data provision, J.U.; data preparation, O.A. and J.P.; software and programming, O.A. and J.P.; field investigation and sampling, O.A., J.U., A.L. and J.P.; visualization, O.A.; writing—original draft preparation, O.A.; writing—review and editing, J.U., A.L. and J.P.; supervision, J.U. and A.L.; project administration, J.U. All authors have read and agreed to the published version of the manuscript.

Funding: Open access funding provided by University of Helsinki. This work has been funded by the public-private partnership grant established for the professorship of forest operation and logistics at the University of Helsinki, grant number 7820148 and by the proof-of-concept-grant by the Faculty of Agriculture and Forestry, University of Helsinki, grant number 78004041.

Acknowledgments: We would like thank Pekka Huuhka for constructing the research sulky and Mikko Leinonen for assisting in the field operations. We would also like to express our gratitude to Finsilva Oyj for providing the access to their forest holdings and related forest inventory databases.

Conflicts of Interest: The authors declare no conflict of interest. The funders had no role in the design of the study; in the collection, analyses, or interpretation of data; in the writing of the manuscript, or in the decision to publish the results.

References

1. Pini, M.; Marucco, G.; Falco, G.; Nicola, M.; Wilde, W.D. Experimental Testbed and Methodology for the Assessment of RTK GNSS Receivers Used in Precision Agriculture. *IEEE Access* **2020**, *8*, 14690–14703. [CrossRef]
2. Kadeřábek, J.; Shapoval, V.; Matějka, P.; Kroulík, M.; Kumhála, F. Comparison of Four RTK Receivers Operating in the Static and Dynamic Modes Using Measurement Robotic Arm. *Sensors* **2021**, *21*, 7794. [CrossRef] [PubMed]
3. Möller, J.J.; Arlinger, J.; Hannrup, B.; Larsson, W.; Barth, A. Harvester data as a base for management of forest operations and feedback to forest owners. In Proceedings of the 4th Forest Engineering Conference: Innovation in Forest Engineering—Adapting to Structural Change, Stellenbosch, South Africa, 5–7 April 2011; Ackerman, P., Ham, H., Elizabeth, G., Eds.; Department of Forest and Wood Science: White River, South Africa, 2011. ISBN 978-0-7972-1284-8.
4. Olivera, A.; Visser, R. Using the harvester on-board computer capability to move towards precision forestry. *N. Z. J. For.* **2016**, *60*, 3–7. [CrossRef]
5. Auat Cheein, F.; Torres-Torriti, M.; Rosell-Polo, J.R. Usability analysis of scan matching techniques for localization of field machinery in avocado groves. *Comput. Electron. Agric.* **2019**, *162*, 941–950. [CrossRef]
6. Kemmerer, J.; Labelle, E.R. Using harvester data from on-board computers: A review of key findings, opportunities and challenges. *Eur. J. For. Res.* **2021**, *140*, 1–17. [CrossRef]
7. Saukkola, A.; Melkas, T.; Riekki, K.; Sirparanta, S.; Peuhkurinen, J.; Holopainen, M.; Hyyppä, J.; Vastaranta, M. Predicting Forest Inventory Attributes Using Airborne Laser Scanning, Aerial Imagery, and Harvester Data. *Remote Sens.* **2019**, *11*, 797. [CrossRef]
8. Noordermeer, L.; Næsset, E.; Gobakken, T. Effects of harvester positioning errors on merchantable timber volume predicted and estimated from airborne laser scanner data in mature Norway spruce forests. *Silva Fenn.* **2022**, *56*, 10608. [CrossRef]
9. Schwarzbach, P.; Michler, A.; Tauscher, P.; Michler, O. An Empirical Study on V2X Enhanced Low-Cost GNSS Cooperative Positioning in Urban Environments. *Sensors* **2019**, *19*, 5201. [CrossRef]
10. Donahue, B.; Wentzel, J.; Berg, R. *Guidelines for RTK/RTN GNSS Surveying in Canada*; Natural Resources Canada: Vancouver, BC, Canada, 2013.
11. Sigrist, P.; Coppin, P.; Hermy, M. Impact of forest canopy on quality and accuracy of GPS measurements. *Int. J. Remote Sens.* **1999**, *20*, 3595–3610. [CrossRef]
12. Naesset, E.; Jonmeister, T. Assessing Point Accuracy of DGPS Under Forest Canopy Before Data Acquisition, in the Field and After Postprocessing. *Scand. J. For. Res.* **2002**, *17*, 351–358. [CrossRef]
13. Murgaš, V.; Sačkov, I.; Sedliak, M.; Tunák, D.; Chudý, F. Assessing horizontal accuracy of inventory plots in forests with different mix of tree species composition and development stage. *J. For. Sci.* **2018**, *64*, 478–485. [CrossRef]
14. Feng, T.; Chen, S.; Feng, Z.; Shen, C.; Tian, Y. Effects of Canopy and Multi-Epoch Observations on Single-Point Positioning Errors of a GNSS in Coniferous and Broadleaved Forests. *Remote Sens.* **2021**, *13*, 2325. [CrossRef]
15. Ordóñez Galán, C.; Rodríguez-Pérez, J.R.; Martínez Torres, J.; García Nieto, P.J. Analysis of the influence of forest environments on the accuracy of GPS measurements by using genetic algorithms. *Math. Comput. Model.* **2011**, *54*, 1829–1834. [CrossRef]
16. Piedallu, C.; Gégout, J.-C. Effects of Forest Environment and Survey Protocol on GPS Accuracy. *Photogramm. Eng. Remote Sens.* **2005**, *71*, 1071–1078. [CrossRef]
17. Valbuena, R.; Mauro, F.; Rodríguez-Solano, R.; Manzanera, J.A. Partial Least Squares for Discriminating Variance Components in Global Navigation Satellite Systems Accuracy Obtained Under Scots Pine Canopies. *For. Sci.* **2012**, *58*, 139–153. [CrossRef]
18. Kabir, M.S.N.; Song, M.-Z.; Sung, N.-S.; Chung, S.-O.; Kim, Y.-J.; Noguchi, N.; Hong, S.-J. Performance comparison of single and multi-GNSS receivers under agricultural fields in Korea. *Eng. Agric. Environ. Food* **2016**, *9*, 27–35. [CrossRef]
19. White, J.C.; Wulder, M.A.; Varhola, A.; Vastaranta, M.; Coops, N.C.; Cook, B.D.; Pitt, D.; Woods, M. A best practices guide for generating forest inventory attributes from airborne laser scanning data using an area-based approach. *For. Chron.* **2013**, *89*, 722–723. [CrossRef]
20. Maltamo, M.; Næsset, E.; Vauhkonen, J. *Forestry Applications of Airborne Laser Scanning: Concepts and Case Studies*; Maltamo, M., Næsset, E., Vauhkonen, J., Eds.; Springer: Dordrecht, The Netherlands, 2014; ISBN 978-94-017-8662-1.
21. Su, Y. *The Use of LiDAR in Multi-Scale Forestry Applications*; University of California: Merced, CA, USA, 2017.
22. Ene, L.T.; Næsset, E.; Gobakken, T.; Mauya, E.W.; Bollandsås, O.M.; Gregoire, T.G.; Ståhl, G.; Zahabu, E. Large-scale estimation of aboveground biomass in miombo woodlands using airborne laser scanning and national forest inventory data. *Remote Sens. Environ.* **2016**, *186*, 626–636. [CrossRef]
23. Noordermeer, L.; Økseter, R.; Ørka, H.O.; Gobakken, T.; Næsset, E.; Bollandsås, O.M. Classifications of Forest Change by Using Bitemporal Airborne Laser Scanner Data. *Remote Sens.* **2019**, *11*, 2145. [CrossRef]
24. Sherba, J.; Blesius, L.; Davis, J. Object-Based Classification of Abandoned Logging Roads under Heavy Canopy Using LiDAR. *Remote Sens.* **2014**, *6*, 4043–4060. [CrossRef]
25. Abdi, O.; Uusitalo, J.; Kivinen, V.-P. Logging Trail Segmentation via a Novel U-Net Convolutional Neural Network and High-Density Laser Scanning Data. *Remote Sens.* **2022**, *14*, 349. [CrossRef]
26. Qian, C.; Liu, H.; Tang, J.; Chen, Y.; Kaartinen, H.; Kukko, A.; Zhu, L.; Liang, X.; Chen, L.; Hyyppä, J. An Integrated GNSS/INS/LiDAR-SLAM Positioning Method for Highly Accurate Forest Stem Mapping. *Remote Sens.* **2017**, *9*, 3. [CrossRef]
27. Kukko, A.; Kaijaluoto, R.; Kaartinen, H.; Lehtola, V.V.; Jaakkola, A.; Hyyppä, J. Graph SLAM correction for single scanner MLS forest data under boreal forest canopy. *ISPRS J. Photogramm. Remote Sens.* **2017**, *132*, 199–209. [CrossRef]

28. Poluzzi, L.; Tavasci, L.; Corsini, F.; Barbarella, M.; Gandolfi, S. Low-cost GNSS sensors for monitoring applications. *Appl. Geomat.* **2020**, *12*, 35–44. [CrossRef]
29. Tsakiri, M.; Sioulis, A.; Piniotis, G. Compliance of low-cost, single-frequency GNSS receivers to standards consistent with ISO for control surveying. *Int. J. Metrol. Qual. Eng.* **2017**, *8*, 11. [CrossRef]
30. Wielgocka, N.; Hadas, T.; Kaczmarek, A.; Marut, G. Feasibility of Using Low-Cost Dual-Frequency GNSS Receivers for Land Surveying. *Sensors* **2021**, *21*, 1956. [CrossRef]
31. Xue, C.; Psimoulis, P.; Zhang, Q.; Meng, X. Analysis of the performance of closely spaced low-cost multi-GNSS receivers. *Appl. Geomat.* **2021**, *13*, 415–435. [CrossRef]
32. Semler, Q.; Mangin, L.; Moussaoui, A.; Semin, E. Development of a Low-Cost Centimetric Gnss Positioning Solution for Android Applications. *Int. Arch. Photogramm. Remote Sens. Spat. Inf. Sci.* **2019**, *XLII-2/W17*, 309–314. [CrossRef]
33. Li, T.; Zhang, H.; Gao, Z.; Chen, Q.; Niu, X. High-Accuracy Positioning in Urban Environments Using Single-Frequency Multi-GNSS RTK/MEMS-IMU Integration. *Remote Sens.* **2018**, *10*, 205. [CrossRef]
34. Yuwono; Handoko, E.Y.; Cahyadi, M.N.; Rahmadiansah, A.; Yudha, I.S.; Sari, A. Assessment of the Single Frequency Low Cost GPS RTK Positioning. *IOP Conf. Ser. Earth Environ. Sci.* **2019**, *280*, 12025. [CrossRef]
35. Janos, D.; Kuras, P. Evaluation of Low-Cost GNSS Receiver under Demanding Conditions in RTK Network Mode. *Sensors* **2021**, *21*, 5552. [CrossRef] [PubMed]
36. Krietemeyer, A.; van der Marel, H.; van de Giesen, N.; Veldhuis, M.-C.T. High Quality Zenith Tropospheric Delay Estimation Using a Low-Cost Dual-Frequency Receiver and Relative Antenna Calibration. *Remote Sens.* **2020**, *12*, 1393. [CrossRef]
37. Jackson, J.; Saborio, R.; Ghazanfar, S.A.; Gebre-Egziabher, D.; Davis, B. *Evaluation of Low-Cost, Centimeter-Level Accuracy OEM GNSS Receivers*; MN/RC 2018-10; University of Minnesota: Minneapolis, MN, USA, 2018.
38. Hauglin, M.; Hansen, E.H.; Næsset, E.; Busterud, B.E.; Gjevestad, J.G.O.; Gobakken, T. Accurate single-tree positions from a harvester: A test of two global satellite-based positioning systems. *Scand. J. For. Res.* **2017**, *32*, 774–781. [CrossRef]
39. Kaartinen, H.; Hyyppä, J.; Vastaranta, M.; Kukko, A.; Jaakkola, A.; Yu, X.; Pyörälä, J.; Liang, X.; Liu, J.; Wang, Y.; et al. Accuracy of Kinematic Positioning Using Global Satellite Navigation Systems under Forest Canopies. *Forests* **2015**, *6*, 3218–3236. [CrossRef]
40. National Land Survey of Finland. Laser Scanning Data 5 p. Available online: https://www.maanmittauslaitos.fi/en/maps-and-spatial-data/expert-users/product-descriptions/laser-scanning-data-5-p (accessed on 6 May 2021).
41. National Land Survey of Finland. NLS Orthophotos. Available online: https://tiedostopalvelu.maanmittauslaitos.fi/tp/kartta?lang=en (accessed on 1 May 2021).
42. U-blox AG. ZED-F9P: U-blox F9 High Precision GNSS Module. Integration Manual. Available online: https://www.u-blox.com/en/docs/UBX-18010802 (accessed on 15 November 2021).
43. U-blox AG. ANN-MB Series: Multi-band, High Precision GNSS Antennas. Data Sheet. Available online: https://www.u-blox.com/sites/default/files/ANN-MB_DataSheet_%28UBX-18049862%29.pdf (accessed on 15 November 2021).
44. U-blox AG. ZED-F9P: Application Note. Available online: https://www.u-blox.com/en/docs/UBX-19009093 (accessed on 15 November 2021).
45. U-blox AG. ZED-F9P Module: U-blox F9 High Precision GNSS Module. Available online: https://www.u-blox.com/en/ubx-viewer/view/ZED-F9P_ProductSummary_UBX-17005151?url=https%3A%2F%2Fwww.u-blox.com%2Fsites%2Fdefault%2Ffiles%2FZED-F9P_ProductSummary_UBX-17005151.pdf (accessed on 1 December 2021).
46. U-blox AG. U-Center: GNSS Evaluation Software for Windows. User Guide. Available online: https://www.u-blox.com/en/docs/UBX-13005250 (accessed on 1 December 2021).
47. ESRI. Lidar Solutions in ArcGIS: Estimating Forest Canopy Density and Height. Available online: https://desktop.arcgis.com/en/arcmap/latest/manage-data/las-dataset/lidar-solutions-estimating-forest-density-and-height.htm (accessed on 10 December 2021).
48. Wilson, J.P. *Environmental Applications of Digital Terrain Modeling*, 1st ed.; Wiley-Blackwell: Hoboken, NJ, USA, 2018.
49. Florinsky, I.V. *Digital Terrain Analysis in Soil Science and Geology*; Academic Press: Oxford, UK; Amsterdam, The Netherlands, 2012; ISBN 978-0-12-385036-2.
50. Dong, P.; Chen, Q. *LiDAR Remote Sensing and Applications*, 1st ed.; CRC Press: Boca Raton, FL, USA, 2017; ISBN 9781482243017.
51. Evans, J.; Hudak, A.; Faux, R.; Smith, A.M. Discrete Return Lidar in Natural Resources: Recommendations for Project Planning, Data Processing, and Deliverables. *Remote Sens.* **2009**, *1*, 776–794. [CrossRef]
52. García, R.; Suárez, J.C.; Patenaude, G. Delineation of individual tree crowns for LiDAR tree and stand parameter estimation in Scottish woodlands. In *The European Information Society*; Cartwright, W., Gartner, G., Meng, L., Peterson, M.P., Fabrikant, S.I., Wachowicz, M., Eds.; Springer: Berlin/Heidelberg, Germany, 2007; pp. 55–85. ISBN 978-3-540-72384-4.
53. ESRI. Creating Intensity Images from Lidar in ArcGIS. Available online: https://desktop.arcgis.com/en/arcmap/latest/manage-data/las-dataset/lidar-solutions-creating-intensity-images-from-lidar.htm (accessed on 12 December 2021).
54. Friedman, J.H. Stochastic gradient boosting. *Comput. Stat. Data Anal.* **2002**, *38*, 367–378. [CrossRef]
55. Salford Systems. Salford Predictive Modeler: Introducing TreeNet® Gradient Boosting Machine. 2019. Available online: https://www.minitab.com/en-us/products/spm/user-guides/ (accessed on 11 December 2021).
56. Swets, J.A. Measuring the accuracy of diagnostic systems. *Science* **1988**, *240*, 1285–1293. [CrossRef]
57. Friedman, J.H. Greedy function approximation: A gradient boosting machine. *Ann. Statist.* **2001**, *29*, 1189–1232. [CrossRef]

58. Hutchinson, M.F. A new procedure for gridding elevation and stream line data with automatic removal of spurious pits. *J. Hydrol.* **1989**, *106*, 211–232. [CrossRef]
59. Burrough, P.A.; McDonnell, R.A. *Principles of Geographical Information Systems*; Oxford University Press: New York, NY, USA, 1998; ISBN 9780198748618.
60. Szypuła, B. Digital Elevation Models in Geomorphology. In *Hydro-Geomorphology—Models and Trends*; Shukla, D.P., Ed.; InTech: Rijeka, Croatia, 2017; ISBN 978-953-51-3573-9.
61. Holpp, M.; Kroulik, M.; Kviz, Z.; Anken, T.; Sauter, M.; Hensel, O. Large-scale field evaluation of driving performance and ergonomic effects of satellite-based guidance systems. *Biosyst. Eng.* **2013**, *116*, 190–197. [CrossRef]
62. Santra, A.; Mahato, S.; Mandal, S.; Dan, S.; Verma, P.; Banerjee, P.; Bose, A. Augmentation of GNSS utility by IRNSS/NavIC constellation over the Indian region. *Adv. Space Res.* **2019**, *63*, 2995–3008. [CrossRef]
63. Brach, M. Rapid Static Positioning Using a Four System GNSS Receivers in the Forest Environment. *Forests* **2022**, *13*, 45. [CrossRef]
64. Wing, M.G. Consumer-Grade GPS Receiver Measurement Accuracy in Varying Forest Conditions. *Res. J. For.* **2011**, *5*, 78–88. [CrossRef]
65. Joyce, M.; Moen, R. *Accuracy of a Modular GPS/GLONASS Receiver*; NRRI/TR-2018/28, 2018, Release 1.0; University of Minnesota Duluth: Duluth, MN, USA, 2018.
66. Konnestad, A.J. *On the Accuracy of GNSS in Forests: A Test of Consumer-Grade GNSS Equipment, Smartphones and Open-Source Postprocessing Software under Forest Canopies, for Mapping of Forest Species*; Norwegian University of Life Sciences: As, Norway, 2018.
67. Pesyna, K.M.; Heath, R.W.; Humphreys, T.E. Centimeter Positioning with a Smartphone-Quality GNSS Antenna. In Proceedings of the 27th International Technical Meeting of the Satellite Division of The Institute of Navigation (ION GNSS+ 2014), Tampa, FL, USA, 8–12 September 2014.
68. Merry, K.; Bettinger, P. Smartphone GPS accuracy study in an urban environment. *PLoS ONE* **2019**, *14*, e0219890. [CrossRef]
69. Ritchie, D.A. *Factors That Affect the Global Positioning System and Global Navigation Satellite System in an Urban and Forested Environment*; East Tennessee State University: Johnson City, TN, USA, 2007.
70. Brach, M.; Stereńczak, K.; Bolibok, L.; Kwaśny, Ł.; Krok, G.; Laszkowski, M. Impacts of forest spatial structure on variation of the multipath phenomenon of navigation satellite signals. *Folia For. Pol.* **2019**, *61*, 3–21. [CrossRef]
71. Pirti, A. Accuracy Analysis of GPS Positioning Near the Forest Environment. *Croat. J. For. Eng.* **2008**, *29*, 189–199.
72. Simwanda, M.; Wing, M.G.; Sessions, J. Evaluating Global Positioning System Accuracy for Forest Biomass Transportation Tracking within Varying Forest Canopy. *West. J. Appl. For.* **2011**, *26*, 165–173. [CrossRef]
73. Yan, F.; Hu, X.; Xu, L.; Wu, Y. Construction and Accuracy Analysis of a BDS/GPS-Integrated Positioning Algorithm for Forests. *Croat. J. For. Eng.* **2021**, *42*, 321–335. [CrossRef]
74. Kobal, M.; Bertoncelj, I.; Pirotti, F.; Dakskobler, I.; Kutnar, L. Using lidar data to analyse sinkhole characteristics relevant for understory vegetation under forest cover-case study of a high karst area in the dinaric mountains. *PLoS ONE* **2015**, *10*, e0122070. [CrossRef]
75. D'Eon, R.G.; Delparte, D. Effects of radio-collar position and orientation on GPS radio-collar performance, and the implications of PDOP in data screening. *J. Appl. Ecol.* **2005**, *42*, 383–388. [CrossRef]
76. Zimbelman, E.G.; Keefe, R.F. Real-time positioning in logging: Effects of forest stand characteristics, topography, and line-of-sight obstructions on GNSS-RF transponder accuracy and radio signal propagation. *PLoS ONE* **2018**, *13*, e0191017. [CrossRef] [PubMed]